

Behavior of Concrete Beams encasing castellated Steel Sections with Different Opening Shapes

Mohammed A. Qasim

Civil Engineering Department, Mustansiriyah University, Baghdad, Iraq
eng.m@uomustansiriyah.edu.iq (corresponding author)

Waleed A. Waryosh

Civil Engineering Department, Mustansiriyah University, Baghdad, Iraq
waleedwaryosh@uomustansiriyah.edu.iq

Received: 8 November 2024 | Revised: 20 November 2024 | Accepted: 1 December 2024

Licensed under a CC-BY 4.0 license | Copyright (c) by the authors | DOI: <https://doi.org/10.48084/etasr.9389>

ABSTRACT

This study investigates the behavior of concrete-encased castellated steel beams featuring various aperture geometries and shear stud connector configurations. Five Composite Castellated Beam (CCB) specimens were tested under two-point loading conditions, including one control specimen with a solid steel section and four specimens with castellated steel beams encased in Normal-Strength Concrete (NSC). The castellated beams featured either Hexagonal (H) or Rectangular (R) openings, and the shear stud connectors provided either Full (F) or Partial (P) interaction between the steel and concrete components. The research objectives were to determine the maximum load capacity for each sample under applied loads, analyze the resulting deformations, and assess the impact of the opening shape and shear connections on the beam performance. The results showed that the H opening improved the load-bearing capacity by 19% and reduced the deflection and horizontal displacement by 21.47% and 12.86%, respectively, compared to the R opening sample. Specimens with F interaction exhibited a higher load capacity and lower deflection and horizontal displacement than those with P interaction. The F configuration increased load tolerance by 2.44% and decreased the deflection and horizontal displacement rates by 4.17% and 5.86%, respectively, relative to the P configuration. The findings demonstrate the influence of aperture geometry and shear connections on the structural performance of concrete-encased castellated steel beams, providing insights for optimizing their design in composite construction.

Keywords- composite castellated beam; hexagonal opening; rectangular opening; full interaction; horizontal displacement

I. INTRODUCTION

Structural engineers have consistently refined the design and functionality of steel structures to achieve enhanced strength, reduced weight, and lower construction costs. A significant advancement in fabricated structural elements is the development of castellated steel beams, which are created by cutting I or H steel sections in a longitudinal zigzag pattern, separating the halves, and then reassembling them. As the depth of a castellated beam increases during manufacturing, its stiffness and strength are enhanced [1, 2].

Authors in [3] examined the flexural performance of composite beams incorporating steel tube sections through various bending tests. The results demonstrated that hollow steel sections with H, square, and R openings consistently maintain the structural service quality of the structures. The experimental results revealed that the performance and angle connection types serve as highly effective shear connectors.

These performed-type shear connectors improved the ultimate load of the composite beams by 6.25–9.74% when compared to the stud shear connectors [4].

Experimental studies have been conducted to analyze the behavior of polymer concrete CCBs featuring different aperture shapes [5, 6]. These studies focused on evaluating the maximum load-bearing capacity and deformation of composite beam specimens. The evaluation covered several factors, including the geometry of the castellated beam apertures and the F or P interaction of shear stud connectors with concrete. The research findings revealed that the H-opening design offered a superior strength capacity and decreased deflection and slide. The F-type interconnections demonstrated an enhanced strength capacity with reduced deflection and slide.

Other researchers have also investigated the impact of the space between the upper and lower portions of asymmetrical castellated steel beams on the web post areas. The results were

obtained from two concentrated load tests performed on four samples. For comparison, the second, third, and fourth specimens were reinforced with RPC, lacing, and deference gaps of approximately 19.1 mm, 38.2 mm, and 57.3 mm, respectively [7, 8]. Five 2-C-shaped beam specimens with varying configurations and web openings were evaluated. This investigation showed that decreasing the number of web holes reduced the bearing strength [9]. The bearing strength increased with an increase in the number of web holes up to a certain point. The stud connectors joined the steel component in the concrete slab. The two-point loading on five simply supported composite beams has been examined [10].

In [11], three specimens were built using castellated steel beams, and two conventional steel beam-constructed specimens served as the controls. One specimen was constructed utilizing a steel castellated beam with an asymmetrical cross-section from two different standard sections (IPE120/HEA120). Experiments demonstrated that CCBs were significantly stronger and stiffer than composite beams made from parent sections [11]. Researchers have conducted asymmetrical experimental studies on RPC-based concrete CCBs and IPE steel. They observed an increase in the ultimate load capacity of the beams by about 10.5% to 19.5% compared to the reference CCB (without reinforcement) [12]. The research analyzed six double-web steel sections from castellated steel beams and non-composite and composite-reinforced concrete deck slabs. The following properties were evaluated: stiffness, flexibility, load at cracking, failure mechanism, load-deflection relationship at midspan, and final strength. For castellation ratios of 0%, 25%, and 50%, the concrete slab increased the ultimate load by 61.1%, 63.3%, and 55.5%, respectively [13, 14]. Scientists have examined the behavior of castellated beams partially covered with concrete. However, the behavior of beams fully encased in concrete remains unstudied.

This research investigates the characteristics of castellated beams completely enclosed in concrete. The investigation focused on analyzing the response of a CCB when subjected to various load intensities. The objectives of this study include examining the structural performance of steel beams, determining their load-carrying capabilities, measuring deflection and lateral displacement under load, and exploring the effects of factors, such as the geometry of openings (H and R) and shear connectors interconnections (F and P).

II. EXPERIMENTAL PART

A. Manufactured Beams with Castellation

Castellated steel beams were manufactured by making longitudinal zigzag cuts along the centerline of a rolled steel I beam. A plasma generator with a computer numerical control was used to execute the cutting process, producing holes with a clean and uniform shape. Once the cutting process was completed, the two pieces of the beam were separated and repositioned. The web pattern's apexes were joined through continuous electric welding of 3 mm thickness, resulting in a castellated steel I-section. This process increased the overall beam height, thereby improving its bending rigidity and section modulus compared to the original rolled I-beam steel section.

B. Specifications and Dimensions of Specimens for Testing

To evaluate the mechanical characteristics of the steel beams, three samples were cut from the castellated beam to estimate the maximum tensile strength, and modulus of elasticity. The castellated cross-section and dimensions are illustrated in Figure 1, with the steel profile dimensions being MB 200 mm × 100 mm × 21.3 mm, in accordance with the ASTM E8/E8M-15a standard [15]. Additionally, Figure 1 shows the resulting H- and R-openings after the welding process. The encasing of the steel beams was performed with Normal Steel Concrete (NCS), and the samples were named as listed in Table I. The names of the samples encode the type of opening (R or H) and the stud interconnection.

TABLE I. TEST SAMPLE DETAILS

No.	Designation of the specimen	Description
1	NSCOF	(reference specimen) CCB encasing with NSC on each section, solid and F.
2	NSCHF	CCB encasing with NSC on each section, opening H and F.
3	NSCHP	CCB encasing with NSC on each section, opening H and P (70% of full).
4	NSCRF	CCB encasing with NSC on each section, opening R and F.
5	NSCRP	CCB encasing with NSC on each section, opening R and P (70% of full).

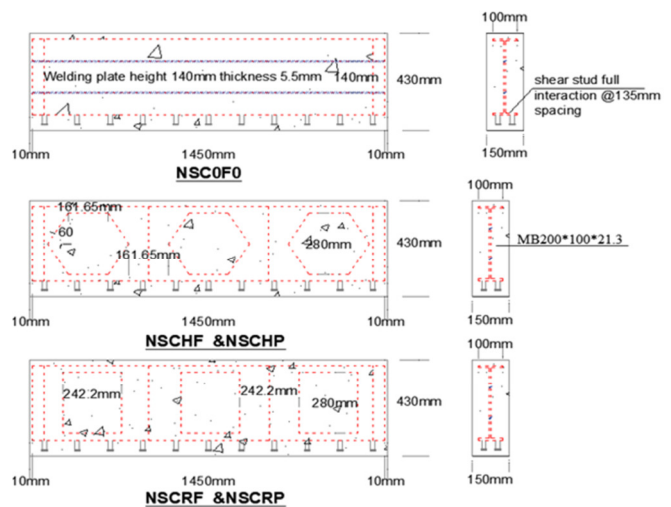


Fig. 1. Cross-sectional profiles of castellated steel beams of samples NSCOF, NSCHF, NSCHP, NSCRF, and NSCRP.

C. Shear Stud Connectors

The shear stud connection was 8 mm in diameter, 40 mm in total height, and 13 mm in upper head diameter. The height-to-diameter ratio was 5 in accordance with the BS 5400-5 code [16]. Table II provides comprehensive information on the specifications and mechanical characteristics of the shear stud connectors. In the case of complete interaction, the shear bolts were spaced 135 mm apart, whereas for P interaction, this distance increased to 190 mm.

TABLE II. GEOMETRY OF SHEAR CONNECTORS AND MECHANICAL PROPERTIES

Actual bar diameter (mm)	8
Actual head stud diameter (mm)	13
Height of the shear connector (mm)	40
Thickness of head stud (mm)	8
Ec (MPa)	205000
Fy (MPa)	280
fu (MPa)	400

D. Materials

The properties of the materials were effectively evaluated using standardized testing methods based on the Iraqi Standard (IQS) and ASTM standards. This research examined a Type I common Portland cement, which was kept dry to be protected from various weather conditions. The cement was found to comply with the Iraqi Standards (No.5/1984) [17] and ASTM-C150-17 [18] based on the test results. Natural sand with a maximum particle size of 4.75 mm was utilized as the fine aggregate in concrete mixtures for all building types after the necessary evaluation. The graded fine aggregate was shown to satisfy the zone specifications of IQS No. 45/1984 [19] and ASTM C128-15 [20]. To adhere to the Iraqi regulations, local gravel was crushed, and various concrete mixtures with a maximum particle size of 12.5 mm were developed. Each piece of crushed gravel was thoroughly cleaned, kept dry for an extended period, and then encased in plastic according to the IQS No. 45/1984 Zone [19]. Tap water was used for mixing and curing all the concrete specimens in this study.

E. Mixing NSC

Table III lists the composition ratios of the NSC utilized in this study.

TABLE III. PROPERTIES OF NSC MIX

water/cement ratio	Cement (kg/m ³)	Water (L/m ³)	Fine aggregate (kg/m ³)	Aggregate (kg/m ³)
0.45	350	180	600	1200

Before mixing the NSC, it was necessary to ensure that the mixer was clean and slightly damp but not wet. The process began by placing gravel and sand into the mixer. One-third of the total water was added to moisten the components for 60 s. Subsequently, the cement was introduced and blended for 30 s. Then, another third of the water was added and mixed for one min. Finally, the remaining water was slowly incorporated and blended for an additional min, resulting in a total mixing duration of 1.5 min. The entire procedure took four min to complete.

III. RESULTS

A universal compression machine with a 3000 kN capacity was employed to evaluate the specimens. For each mix type, the results were based on the average of three samples. Table IV contains the detailed specifications of the control specimens. The compression, modulus of rupture, splitting tensile strength, and modulus of elasticity were estimated following the BS 1881-116:1983 [21], ASTM C293/C293M-16

[22], ASTM C496/C496M-17 [23], and ASTM C469-02 standards [24], respectively.

TABLE IV. THE SPECIFICATIONS FOR THE CONTROL SPECIMENS

Test classification	Quantity and shape of specimens	Specimen's dimensions (mm)	Average estimated value
Compression	3 cubes	100×100×100	25 MPa
Modulus of rupture	3 prisms	100×100×500	3.25 MPa
Splitting tensile strength	3 cylinders	100×200	2.5 MPa
Modulus of elasticity	3 cylinders	150×300	26.6 GPa

A. Load – Deflection

The bending characteristics of the specimens were investigated under static load conditions. Figure 2 illustrates the load-deflection curves for the tested samples at the midspan throughout each loading phase until failure. All specimens underwent failure testing, resulting in concrete breakdown due to crack propagation. The samples displayed linear behavior from zero to the initial concrete crack, varying based on the concrete type, interaction level, and steel beam opening shape. After the inflection point, the specimen behavior becomes nonlinear due to changes in the modulus of elasticity caused by increased load, which leads to higher strain, subsequently reducing the elasticity modulus and decreasing specimen stiffness. As the load increased, the load-deflection slope decreased, indicating a reduction in specimen stiffness owing to the greater load and deflection. The highest deflection value was observed at the midspan. The CCB beam was evaluated using the reference specimen NSCOF, a solid web without holes, made of NSC, and equipped with several stud shear connectors. The maximum load capacity reached 405 kN with a corresponding midspan deflection of 22 mm. NSCOF exhibited linear behavior from zero to 90 kN, the load at which the first crack appeared. Specimen NSCHF demonstrated a load capacity of 500 kN, but its strength and maximum deflection matched those of specimen NSCOF.

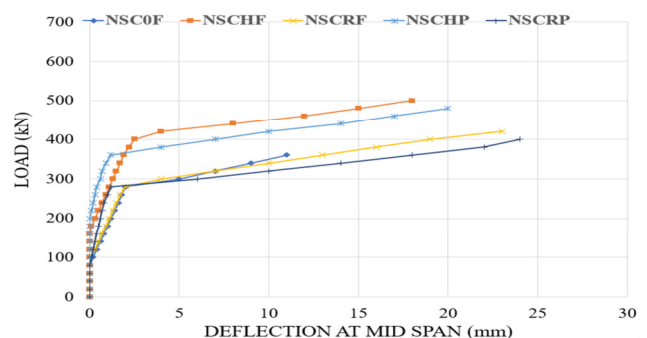


Fig. 2. Load-deflection curves at midspan.

B. Load - Horizontal Displacement

Despite the presence of numerous shear stud connections designed to unite dissimilar materials, like steel and concrete, into a single functional unit, lateral movement still occurs at the interface. The behavior of this horizontal displacement is

portrayed in Figure 3 for each test specimen. The distribution of lateral movement is symmetrical around the center point (midspan) and demonstrates sign reversal. The maximum horizontal displacement ranges from 4.2 to 5.12 mm, for the samples with F and P shear connector interactions. This movement was the result of the applied force.

In the directions of shear flow or shear load, the load-horizontal movement behavior at the mid-span was zero. Initially, when the load was applied, the horizontal movement was negligible. However, as the load increased, causing more shear flow, the movement also increased. The presence of P shear connectors resulted in greater horizontal movement compared to the F shear connectors due to a more distributed shear flow, which induces horizontal movement at the interface when friction is present. This friction force, which acts in the direction opposite to the shear flow, contributes to an increase in the horizontal movement value.

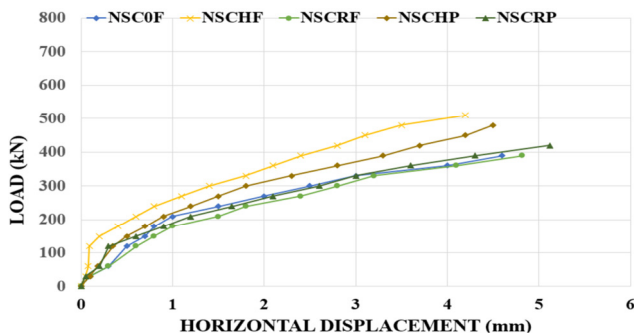


Fig. 3. Load-horizontal displacement curves.

C. Crack Style and Failure Mode

NSC is characterized by its low strain resistance due to its brittle nature. During flexural testing, cracks formed and spread when the stress induced by the applied load in the tensile area exceeded the modulus of rupture. As the applied load approaches the threshold for the initial fracture, the internal stress within the tensile zone of the concrete approaches the modulus of the rupture value.

The initial crack load is influenced by various factors, including the shape and compressive strength of the concrete components. The horizontal movement that amplified the deflection and inhibited the convergence of the concrete and steel sections resulted in a load during the P shear connectors that induced an initial fracture at a lower magnitude compared to a complete F interaction.

Figure 4 illustrates the failure modes and crack propagations for all the CCB specimens. No instances of pull-out were observed.

IV. DISCUSSION

This section provides insights based on the experimental results and observations from the parametric studies conducted in this research. Table V presents a comparative analysis of the specimens categorized according to their opening types (R and H). Figures 5 and 6 show the comparisons of the specimens. The results indicated that larger openings had a significant

impact on the overall strength and load-bearing capacity of the section. This is attributed to the fact that the diagonal span between the edges of an R-type opening exceeds that of an H-type opening.

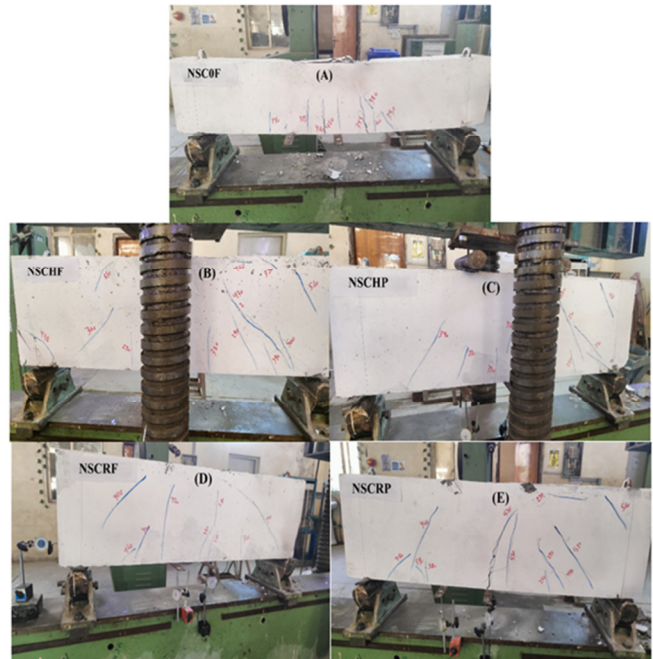


Fig. 4. CCBs at failure stage: (A) NSCOF, (B) NSCHF, (C) NSCHP, (D) NSCRF, and (E) NSCRP.

TABLE V. EFFECT OF THE OPENING FORM ON ULTIMATE LOAD, DEFLECTION, AND HORIZONTAL MOVEMENT OF CCBs

Sample	NSCHF	NSCOF	NSCHF	NSCRF
Ultimate load (kN)	500	405	500	420
% Increase in ultimate load	23.5	-	19.05	-
Max midpoint deflection (mm)	18	22	18	23
% Reduction in midpoint deflection	18.2	-	21.74	-
Max horizontal displacement (mm)	4.2	4.6	4.2	4.82
% Reduction in horizontal displacement	8.7	-	12.86	-

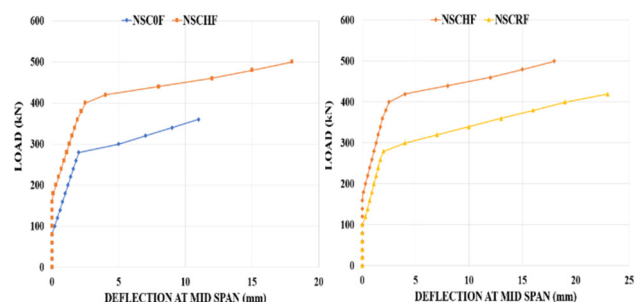


Fig. 5. Load-deflection curves at midspan of NSCOF, NSCHF, and NSCRF samples.

During the construction of the CCBs, the P and F shear connectors regulated the deflection at the midspan and the horizontal movement. The influence of the shear connectors on

the CCB characteristics is presented in Table VI. Figures 7 and 8 demonstrate the comparisons between the specimens. When the castellated steel component fully interacts with concrete, the system operates as a unified entity. F results in additional shear stud connectors that minimize the horizontal movement and deflection. This enhances the capacity of the composite beam compared to a P system by reducing the shear flow transfer between the contacting surfaces of the shear connectors.

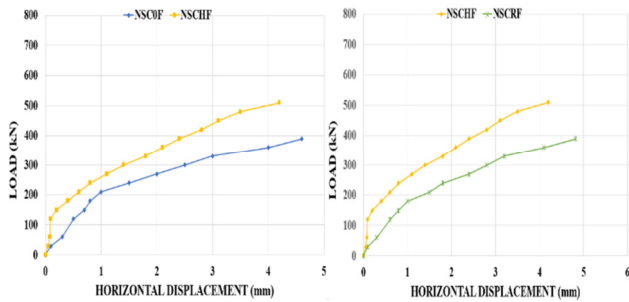


Fig. 6. Load-horizontal displacement curves of NSC0F, NSCHF, and NSCRF samples.

TABLE VI. INFLUENCE OF SHEAR CONNECTORS ON ULTIMATE LOAD, DEFLECTION, AND LATERAL MOVEMENT OF CCBS

Sample	NSCHF	NSCHP	NSCRF	NSCRP
Ultimate load (kN)	500	470	420	410
% Increase in ultimate load	6.38	-	2.44	-
Max midpoint deflection (mm)	18	20	23	24
% Reduction in midpoint deflection	10	-	4.17	-
Max horizontal displacement (mm)	4.2	4.5	4.82	5.12
% Reduction in horizontal displacement	6.67	-	5.86	-

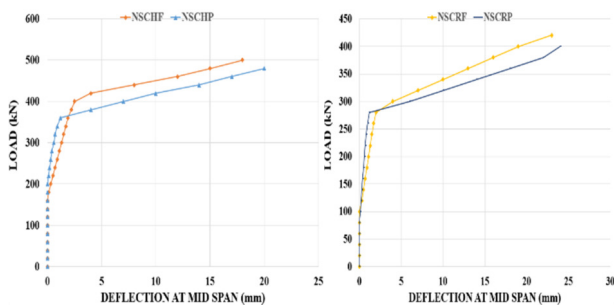


Fig. 7. Load-horizontal displacement curves of NSCHF, NSCRF, NSCHP, and NSCRP samples.

V. CONCLUSIONS

The two most important factors influencing the sectional characteristics of the Composite Castellated Beams (CCBs) were the opening form and shear stud. The experimental examination of the concrete beam encasing the castellated steel section yielded interesting conclusions.

The Rectangular (R) openings in the specimens restrict the load-bearing capacity of the CCBs because of the larger horizontal distance between the opening edges compared to the Hexagonal (H) openings. The experimental results indicated

that vertical and oblique cracks became more prevalent as the number of cracks between the edges increased.

Additionally, a cohesive structure resulted from the complete interaction between the concrete and shear studs at the CCB base. Complete engagement was achieved with a greater number of shear stud connectors, resulting in a reduced shear flow transmission across the contact surfaces of the shear connections.

The H openings were found to increase the ultimate load, while reducing the deflection and horizontal displacement. Compared to the control sample (solid without openings), there was an approximate 23.5% increase, and a 19.05% increase compared to the R-opening sample in terms of ultimate load. The mid-displacement decreased by about 18.2% and 21.74%, respectively. The horizontal displacements were reduced by roughly 8.7% and 12.86%, respectively.

Finally, the analysis of the results indicated that for the H-opening sample with Full (F) stud connector interaction, the load-bearing capacity increased by approximately 6.38% compared with the respective sample with the H opening but with Partial (P) interaction. The deflection and horizontal displacement percentages decreased by approximately 10 and 6.67%, respectively. Regarding the samples with the R opening and F interaction, the load-bearing capacity increased by approximately 2.44% compared to the respective sample with the R opening but with P interaction. The midspan deflection and horizontal displacement percentages decreased by approximately 4.17% and 5.86%, respectively.

REFERENCES

- [1] A. J. Mehetre, R. S. Talikoti, and P. B. Sonawane, "Experimental Research on Equivalent Rectangular Opening Castellated Beam with Fillet Corner," *International Journal of Recent Technology and Engineering*, vol. 8, no. 5, pp. 5415–5420, 2020, <https://doi.org/10.35940/ijrte.E7103.018520>.
- [2] A. I. Khaleel and M. F. K. AL-Shamaa, "Experimental Investigation on the Structural Behavior of Double Channel Castellated Steel Beams," *E3S Web of Conferences*, vol. 318, 2021, Art. no. 03009, <https://doi.org/10.1051/e3sconf/202131803009>.
- [3] H. A. Ammar and A. J. H. Alshimmeri, "A Comparison Study between Asymmetrical Castellated Steel Beams Encased by Reactive Powder Concrete with Laced Reinforcement," *Key Engineering Materials*, vol. 895, pp. 77–87, 2021, <https://doi.org/10.4028/www.scientific.net/KEM.895.77>.
- [4] A. A. Hussein and A. J. H. Alshimmeri, "Comparative Study of Structural Behavior for Asymmetrical Castellated (Concavely - Curved Soffit) Steel Beams with Different Strengthening Techniques," *Key Engineering Materials*, vol. 895, pp. 177–189, 2021, <https://doi.org/10.4028/www.scientific.net/KEM.895.177>.
- [5] H. S. Al-Mawashee and M. A.-A. Al-Kannoon, "Flexural Strength of Castellated Beams with Corrugated Webs," in *Journal of Physics: Conference Series, 3rd International Scientific Conference of Engineering Sciences and Advances Technologies*, Iraq, vol. 1973, Aug. 2021, Art. no. 012213, <https://doi.org/10.1088/1742-6596/1973/1/012213>.
- [6] I. Barkiah and A. R. Darmawan, "Comparative analysis of the flexural capacity of conventional steel beams with Castellated beams," in *IOP Conference Series: Earth and Environmental Science, 3rd International Seminar on Livable Space*, Jakarta, Indonesia, vol. 780, May 2021, Art. no. 012013, <https://doi.org/10.1088/1755-1315/780/1/012013>.
- [7] I. Barkiah, A. R. Darmawan, and M. F. Dziry, "Pengaruh Sudut Bukaian Heksagonal Terhadap Kapasitas Geser Castellated Steel Beam," *Jurnal*

- Teknologi Berkelanjutan*, vol. 10, no. 02, pp. 55–64, Oct. 2021, <https://doi.org/10.20527/jtb.v10i02.201>.
- [8] G. Zhang *et al.*, "Reinforced concrete deep beam shear strength capacity modelling using an integrative bio-inspired algorithm with an artificial intelligence model," *Engineering with Computers*, vol. 38, no. 1, pp. 15–28, Apr. 2022, <https://doi.org/10.1007/s00366-020-01137-1>.
- [9] H. W. Al-Thabhawee, "Experimental investigation of composite steel–concrete beams using symmetrical and asymmetrical castellated beams," *Curved and Layered Structures*, vol. 9, no. 1, pp. 227–235, Jan. 2022, <https://doi.org/10.1515/cls-2022-0019>.
- [10] A. M. Ibrahim, W. D. Salman, and F. M. Bahlol, "Flexural Behavior of Concrete Composite Beams with New Steel Tube Section and Different Shear Connectors," *Tikrit Journal of Engineering Sciences*, vol. 26, no. 1, pp. 51–61, Mar. 2019, <https://doi.org/10.25130/tjes.26.1.07>.
- [11] M. A. Gulam and A. J. H. AlShimmeri, "Structural Behavior Castellated 2C Cold-Formed Steel Beams," *Journal of Engineering*, vol. 30, no. 05, pp. 151–171, May 2024, <https://doi.org/10.31026/j.eng.2024.05.10>.
- [12] I. Al-Salmani, Z. Al-Azawi, and J. Al-Esawi, "Strengthening of Composite Castellated Beams Web with Corrugated Carbon Fiber Reinforced Polymer Struts," *Key Engineering Materials*, vol. 870, pp. 49–60, 2020, <https://doi.org/10.4028/www.scientific.net/KEM.870.49>.
- [13] N. Y. Abbas and A. J. H. Alshimmeri, "Flexural Behavior of a Composite Concrete Castellated Double Channel Steel Beams Strengthening with Reactive Powder Concrete," *Tikrit Journal of Engineering Sciences*, vol. 31, no. 2, pp. 28–42, Apr. 2024, <https://doi.org/10.25130/tjes.31.2.4>.
- [14] F. A. Abass and A. M. Al-Khekany, "Effect of Concrete Slab on Built-up Double Web Castellated Steel Beam under Combined Flexural and Torsion Load," *Salud, Ciencia y Tecnología - Serie de Conferencias*, vol. 3, pp. 840–840, Jan. 2024, <https://doi.org/10.56294/sctconf2024840>.
- [15] *ASTM E8/E8M-15a: Standard Test Methods for Tension Testing of Metallic Materials*. West Conshohocken, PA, USA: ASTM International, 2015.
- [16] *BS 5400-5:1979 - Steel, concrete and composite bridges - Code of practice for design of composite bridges*. UK: British Standards Institution, 1979.
- [17] *Iraqi Specifications No. 5, Portland Cement*. Baghdad, Iraq: Central Organization for Standardization and Quality Control, 1984.
- [18] *ASTM C150/C150M-17: Standard Specification for Portland Cement*. West Conshohocken, PA, USA: ASTM International, 2017.
- [19] *Iraqi Specifications No. 45, Aggregate from Natural Sources for Concrete and Construction*. Baghdad, Iraq: Central Organization for Standardization and Quality Control, 1984.
- [20] *ASTM C128-15: Standard Test Method for Relative Density (Specific Gravity) and Absorption of Fine Aggregate*. West Conshohocken, PA, USA: ASTM International, 2015.
- [21] *BS 1881-116:1983 - Testing concrete - Method for determination of compressive strength of concrete cubes*. UK: British Standards Institution, 1983.
- [22] *ASTM C293/C293M-16: Standard Test Method for Flexural Strength of Concrete (Using Simple Beam With Center-Point Loading)*. West Conshohocken, PA, USA: ASTM International, 2016.
- [23] *ASTM C496/C496M-17: Standard Test Method for Splitting Tensile Strength of Cylindrical Concrete Specimens*. West Conshohocken, PA, USA: ASTM International, 2017.
- [24] *ASTM C469-02: Standard Test Method for Static Modulus of Elasticity and Poisson's Ratio of Concrete in Compression*. West Conshohocken, PA, USA: ASTM International, 2002.